Operation of an Electromagnetic Trigger with a Short-circuit Ring

Dejan Križaj[1*], Zumret Topčagić[1], and Borut Drnovšek[1,2]
[1]Faculty of Electrical Engineering, University of Ljubljana, Ljubljana, Slovenia, [2]RC NELA, Izlake, Slovenia
*Corresponding author: Tržaška 25, 100 Ljubljana, Slovenia, dejan.krizaj@fe.uni-lj.si

Abstract: Numerical simulation of an electromagnetic trigger with a short-circuit ring is presented. The main goal of inclusion of a short-circuit ring in an electromagnetic trigger is to develop an element suitable for use in a circuit breaker with capabilities of selective switching. The main problem to be solved is vibration of a moving contact due to zero electromagnetic force between the anchor and the core at zero driving current . Inclusion of a short-circuit ring into the core results in induction of current in the ring during flux change. This current produces magnetic field that superimposes onto the main field and results in non-zero force between the anchor and the core during zero driving current in the windings. Saturation of magnetic material at increased driving current was taken into account resulting "saturating" force on a striker pin at increased current amplitudes. Nevertheless, numerical simulation reveals that inclusion of a short circuit ring does not significantly decrease the maximal force and that it effectively reduces vibrationy of a moving contact.

Keywords: electromagnetic trigger, short-circuit ring, numerical simulation, circuit breaker.

1. Introduction

Electromagnetic trigger is an essential constitutive part of circuit breakers, devices used to disconnect the load from electric appliance in case of an overload or short-circuit currents. The main parts of the trigger are presented in figure 1 and consist of the core, the yoke, the anchor and the striker pin. The trigger is supposed to operate at 6.25 times the nominal current. The trigger shown in figure 1 has seven windings and is intended for use in a circuit breaker declared for nominal current of 32 A. This means that the trigger should start to operate at about $32 \times 6.25 \times 7 = 1400$ ampere windings. At this condition the electromagnetic force between the anchor and the core should be sufficient to move the anchor toward the core surpassing the force of the spring. The striker pin is pushed by the anchor and if the force (read the current in the winding) is sufficiently strong it switches off the moving contact disconnecting the main current path.
Several parts of the device should be optimized for optimal device operation. For instance, the cross-section area of the yoke has to be sufficient not to cause yoke saturation at large currents. This would result in effective increase of the air gap and reduced magnetic flux through the core reducing the force between the anchor and the core. Thicker cross-section would result in loss of material and unnecessary increased cost.

Classic circuit breakers (MCB) should disconnect in the case of short circuit currents at times shorter than 100 ms. In most cases the disconnection occurs already at times shorter than 10 ms which is already in the first half of the period of the sinusoidal driving current. However, in this investigation we would like to optimize the trigger for operation in a selective MCB where required short circuit disconnection should occur in time not shorter than 10 ms and no longer than 300 ms. Selective circuit breaker thus ensures certain time delay of the disconnection. During the first half period the electromagnetic trigger should disconnect the main contact and redirect the current to a secondary (auxiliary) branch with a series connection of a resistor and a bimetal. The resistor of appropriate value limits the current to about 400 A and deforms the bimetal that completely disconnects the load in time that should be shorter than 300 ms.

The main problem with this type of construction of the selective circuit breaker is vibration of a movable contact (not shown in the figure) that is vibrating with twice the frequency of the current signal. At each half-period, when the sinusoidal current goes through zero the force between the core and the anchor diminishes. At this moment the opposing force of a spring and the force of the moving contact cause a collision between the fixed and the moving contact. Such undesired vibrations may result in undesired welding of the contacts. One of possible solutions to avoid this

effect is to implement a copper ring in a core as also presented in a cross-section of a device in figure 1. The expected function of a copper ring is as follows: the alternating current in the winding causes changing magnetic flux in the core and the anchor and thus also through the copper ring. In the ring the induced field is generated in a circular direction. The ring is highly conductive thus induced electric field causes Ohmic current flow in the ring. According to Lentz law its direction is such that the magnetic field it generates opposes the one that caused it. Largest induced field in the ring occurs at largest time change of the current in the winding which is for sinusoidal current at the moment the current changes sign. Thus, at time the current in the winding is zero the induced field in the ring and thus the induced current and with this current influenced magnetic field is largest and results in non-zero magnetic force between the core and the anchor, just what it was sought.

Short circuit rings have been previously successfully used for a similar purpose as shading coils for single phase magnets as explained in [1] and analyzed as magnetic circuits in [2]. Some simulation attempts of circuit breakers either as circuit models [3] or numerical finite elements analysis [4, 5, 6, 7] however, no numerical simulation study of circuit breakers with a short circuit ring has been found.

The motivation of this investigation was to use numerical simulation to model electromagnetic trigger with and without inclusion of a short circuit ring, to analyze in detail the operation of the device and optimize its position and geometry. An important requirement for numerical simulation was also to take into account adequate material properties, in particular the nonlinear B-H characteristics of the ferromagnetic parts of the trigger. This step is important as device is supposed to operate at large magnetic voltages (ampere windings) where magnetic saturation of some parts of the structure is expected to occur.

2. Design of a structure used in numerical simulation

Figure 1 presents a cross-section of the analyzed structure. Basic elements of the trigger are the core, the anchor, the yoke and the striker pin. The device shown in figure 1 is assumed to have rotational symmetry although in practice all parts except the yoke are rotationally symmetrical. The yoke has a U form with rectangular cross-section and is on one side riveted to the core. Due to numerical simulation in axial symmetry the cross-section was artificially increased to fit the cross-section area of the 3D device.

On the other side of the yoke is an air gap between the yoke and the anchor. A thin plastic tube is used to separate the yoke from the anchor and at the same time facilitates proper movement of the anchor. The thickness of the wall of the tube should also be very small in order to reduce the air gap between the yoke and the anchor and reduce stressing of magnetic field. On the other hand it needs to be thick enough to sustain the mechanical forces. A spring is pushing the striker pin toward the anchor resulting in an initial air gap between the core and the anchor of about 2.5 mm.

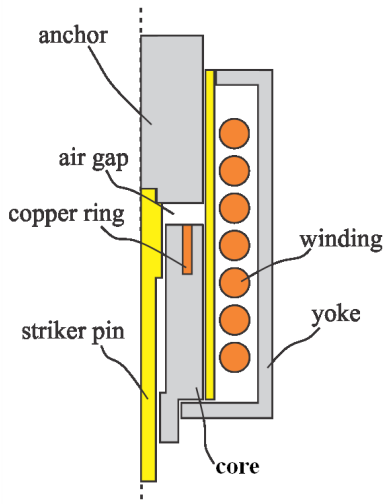

Figure 1. Cross section of a simulated structure with description of constitutive parts.

3. Use of COMSOL Multiphysics

3.1 Equations, materials and boundary conditions

Comsol Multiphysic ver. 4.2a was used for numerical simulation. AC/DC module enables use of several possible sets of differential equations of electromagnetics. For our case time domain simulation of magnetic field in the form of Ampere's law was used:

$$\sigma \frac{\partial \boldsymbol{A}}{\partial t} + \nabla \times \boldsymbol{H} = \boldsymbol{J}_e \qquad (1)$$

where σ is specific resistivity and $\boldsymbol{J}_e$ is external current density $\boldsymbol{A}$ is the magnetic vector potential and $\boldsymbol{H}$ is magnetic field vector. Magnetic flux density $\boldsymbol{B}$ and magnetic field vector are related to magnetic vector potential $\boldsymbol{A}$ through $\boldsymbol{B} = \nabla \times \boldsymbol{A}$ and $\boldsymbol{B} = \mu \boldsymbol{H}$ where μ is permeability (matrix). In case of magnetic materials with nonlinear properties (as will be used in our case for ferromagnetic materials) the relation between *B* and *H* can be expressed with tabulated values or with analytical expression. In our case a built-in *B*(*H*) characteristic for soft iron has been found adequate for modeling magnetic material properties of the core, anchor and the yoke.

Electric field and magnetic and electric potentials are related through

$$\boldsymbol{E} = -\nabla V - \frac{\partial \boldsymbol{A}}{\partial t}. \qquad (2)$$

Also, electrical material properties for the copper winding and the copper ring were taken from the program built-in library.

Since the yoke assures that the core and the anchor are (with a small air gap) magnetically "closed" it is sufficient to surround the simulated structure with a relatively small surrounding air region with zero magnetic vector potential at its boundaries.

A sinusoidal current of a form

$$i(t) = I_0 \sin(2\pi f t) \qquad (3)$$

was imposed to the winding, where I_0 is the amplitude and f the frequency of the applied signal (50 Hz). The force between the anchor and the core was calculated using a built-in approach of a Maxwell stress-tensor $\boldsymbol{T}$ that calculates the surface force by integration of $\boldsymbol{T}$ from calculated magnetic flux density $\boldsymbol{B}$ and magnetic field vector $\boldsymbol{H}$ [8].

3.2 Meshing and solving strategy

Due to 2D axial symmetric simulation a relatively dense mesh could be used for simulation without a fear of a too large number of mesh points and consequently solution times. Typical number of mesh points was 28150. A *Time Dependent simulation* (study) and *Magnetic Fields(mf)* physics was chosen. In the *Magnetic fields(mf)* settings we used two *Ampere´s Law* sections. One is used for the linear materials including a surrounding air region while the second is used for nonlinear parts (anchor, yoke and core) of the simulation structure. In *Ampere´s Law* settings a *Gauge Fixing for A-Field* was selected**.** This approach consumes more computational memory but helps in the convergence of the model as well as accuracy of the solution. *Mesh settings* was set to *Maximum element size* =0.007 in the *Size 1* settings of the *Free Tetrahedral 1* section. In the *Size* settings of the *Mesh* section *Maximum element size* was set to 0.03. *Absolute tolerance* in the *Time Dependent Solver 1* settings for the first variable was set to Unscaled /1e-5 and for the second to Unscaled/8e-3. *Maximum BDF order* in *Time stepping method* solver was set to 2. Lower maximum BDF order speeds up the computation. In the *Time Dependent Solver 1* settings we selected *Direct Solver* method of computation. Direct solver (in our case MUMPS) is more robust and hence a better choice for solving highly nonlinear problems.

In the *Fully Coupled 1* settings in the *Time Dependent Solver 1* section for Linear solver was selected *Direct* option, for Jacobian update was selected *On every iteration* option and *Maximum number of iteration* was set to 25. A higher maximum number of iterations minimizes the risk that the nonlinear solver will terminate prematurely due to the high nonlinearity.

4. Results

4.1 Without a cooper ring

First simulations were performed without inclusion of a copper ring and material nonlinearity. This step facilitates solving strategy as well as understanding of device operation by discriminating the effects due to nonlinearities and due to a copper ring. For these simulations the magnetic properties of ferromagnetic materials were set to relative permeability of 1000. Figure 2 presents absolute values of magnetic flux density (in colours) for rms currents of 72 A and 200 A. In both cases the magnetic flux density is increased in the core and especially in a yoke close to the core. The calculated magnetic flux density is above the value of saturation of soft iron so it is expected that in simulations with proper inclusion of magnetic properties (tabulated) B(H) values for soft iron these regions would be in saturation or

close to it.

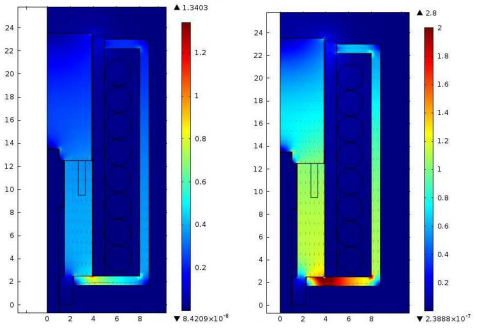

Figure 2:Absolute value of magnetic flux density at the current of a) 72A and b) 200 A. (the material properties of the ring were the same as for soft iron)

In comparison with figure 2, figure 3 presents results for the same imposed current values but with inclusion of magnetic properties of ferromagnetic materials (tabulated B(H) values). In this case the magnetic flux density is quite similar for 75 A rms but quite different for 200 A rms. In the latter case a small part of the yoke is in saturation. This results in increased magnetic resistance of this part of the magnetic circuit which can be also modeled by an effectively increased air gap. A consequence is decreased magnetic flux density in the core also resulting in reduced force between the anchor and the core compared to the former case.

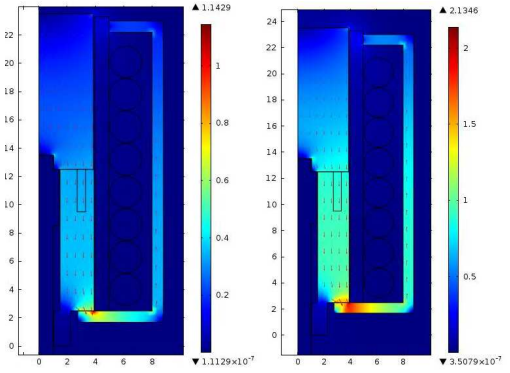

a) b)

Figure 3:Absolute value of magnetic flux density at the rms current of a) 72 A and b) 200 A.

Figure 4 presents time evolution of the force between the anchor and the core for increased current amplitudes as a function of time. In these simulations nonlinear B(H) curve was taken into account for ferromagnetic materials. As expected, the force is sinusoidal as the applied current signal but with doubled frequency of the applied signal. However, the sinusoidal shape is deformed for larger imposed currents which are a clear consequence of increased saturation of the ferromagnetic materials at larger currents. Without saturation effect the force should increase as a square of the imposed current while it is obvious that in case of saturation the force slowly saturates as well.

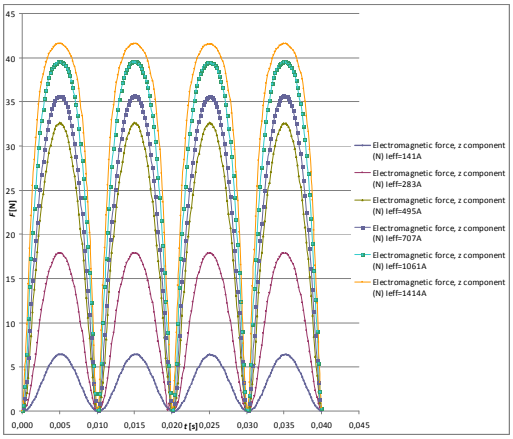

Figure 4: Force as a function time for rms values of alternating currents: 141 A, 283 A, 495 A, 707 A, 1061 A, 1414 A.

4.2 With a cooper ring

As said in introduction, one of the unwanted effects in design of a selective electromagnetic trigger is the vibration of the anchor due to the fact that the force is zero in each half period of the applied signal (see Figure 4). One of possible solutions is to insert a cooper ring inside the core. Cooper is not ferromagnetic but is a very good conductor of electric current. One of the consequences of inserted cooper ring is that due to the decreased cross-section area of the ferromagnetic at the location of the cooper ring the magnetic flux density in this region is increased and it goes into saturation sooner than in the case there was no ring (Figure 5). This is not an advantage as the total magnetic flux is decreased and the force between the anchor and the core is decreased as well. However, time change of the flux through the ring induces electric field inside the ring which drives the

induced (short-circuit) current with such a direction that the magnetic field it produces opposes the one that creates it (Lentz law). This is clearly seen in Figure 6 presenting induced current in the ring and force on an anchor for a sinusoidal driving current. Induced current and driving current are in phase shift for about a quarter of a period, the induced current being large at the moment of maximal time change of the driving current. The induced current creates its own magnetic field in its vicinity and superimposes to the magnetic field created by the driving current.

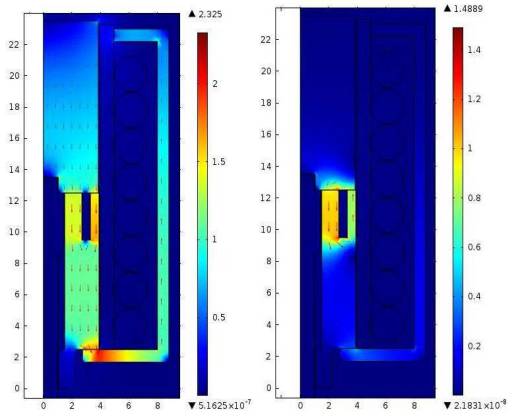

Figure 5: Absolute value of magnetic flux density I_{RMS}=283A after a) 35 ms and after b) 40 ms.

Result of superposition of magnetic fields is nonzero flux through the anchor at the moment when the driving current crosses zero resulting in nonzero force between the anchor and the core. The magnitude of this non-zero (minimal) force can be to some extend tuned by optimizing the position and the geometry of the cooper ring. Also, induced current in the ring is not completely sinusoidal as the driving current. This is a consequence of nonlinearities that occur due to saturation effects which decrease (not increase to the same extent) the flux and thus the force.

Figure 7 presents a comparison of maximal force for various rms currents for a structure with and without a cooper ring. Simulations reveal that due to material saturations effects also the force saturates. Furthermore, inclusion of the cooper ring does not significantly reduce the maximal force but it increases the minimal force, just what was the intention of its function.

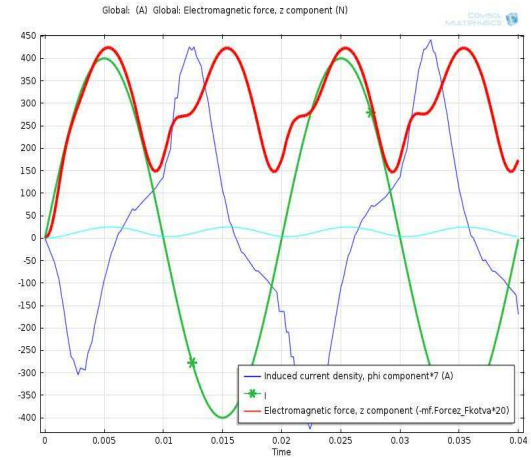

Figure 6: Current (green) and force on an anchor in axial direction (red) as a function of time. In blue is induced current in the copper ring. The force and the induced current are scaled (as seen in the legend).

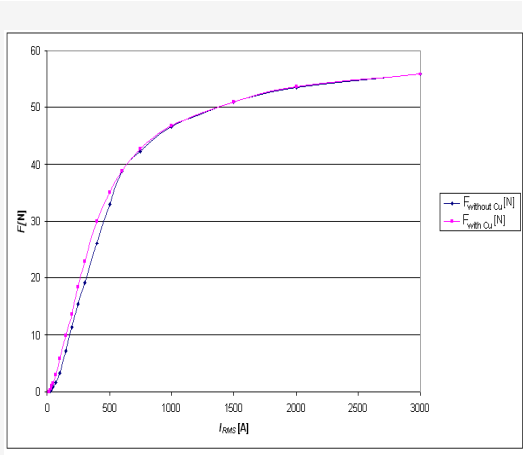

Figure 7: Maximal force as a function of rms current for structure without a cooper ring (blue) and with a ring (red line).

6. Conclusions

Numerical simulations of an electromagnetic trigger have been performed in order to optimize the trigger for operation as a selective trigger. During this operation unwanted vibrations occur between the fixed and the moving contact. Numerical simulations reveal that inclusion of a cooper ring into the core reduce the vibrations in particular due to a non-zero force that occurs due to induced current in the cooper ring. Further optimizations are possible by optimizing the position and geometry of the ring.

7. References

1. H. C. Roters, *Electromagnetic devices*, 463-481. John Wiley and Sons, New York (1941)
2. C. T. Evans, Shading Coil Calculations for Single-Phase Magnets, *Transactions of American Institute of Electrical Engineers*, **66**, 134-138, (1947)
3. J-R. R. Ruiz, A. G. Espinoza, A Novel Parametric Model for AC Contactors, *IEEE Transactions on Magnetics*, **44 (9)**, 2215-2218 (2008)
4. M. Lindmayer, H. Stammberger, Application of Numerical Field Simulations for Low-Voltage Circuit Breakers, *IEEE Transactions on Components, Packaging and Manufacturing Technology – Part A*, **18 (3)**, 708-717 (1995)
5. Li Erping P. M. McEwan, Analysis of a Cicrcuit Breaker Solenoid Actuator System using the Decoupled CAD-FE Integral Technique, *IEEE Transactions on Magnetics*, **28 (2)**, 1279-1282 (1992)
6. S. Ito, Y. Takato, Y. Kawase, T. Ota, Numerical Analysis of Elecctromagnetic Forces in Low Voltage AC Circuit Breakers using 3-D Finite Element method into account Eddy Currents, *IEEE Transactions on Magnetics*, **34 (5)**, 2597-2600 (1998)
7. B. Drnovšek, D. Križaj, Numerical Simulation and Design of a Selective Electromagnetic Breaker, *Electrotechnical Review*, Slovenia, **74 (5)**, 273-278 (2007)
8. *AC/DC Module – Users Guide, Comsol Ver 4.2a*, Comsol Inc. (2011)